

ORIGINAL PAPER

T. Yazawa · J. L. Wilkens
H. E. D. J. ter Keurs · M. J. Cavey

Structure and contractile properties of the ostial muscle (musculus orbicularis ostii) in the heart of the American lobster

Accepted: 10 August 1999

Abstract “Venous” blood enters the crustacean heart through bivalved ostia. Each ostium is a discrete anatomical unit that remains functional even when isolated from the heart. Muscle fibers produce overshooting action potentials that have a plateau of variable duration in response to nervous drive from the cardiac ganglion or during trains of electrical stimuli. Contractions show summation and facilitation when stimulated by trains of stimuli delivered at rates greater than 0.5 s^{-1} and 0.2 s^{-1} , respectively. Contraction amplitude increases with stimulating impulse frequency and train duration. Maximum force occurs at 1.2 times the slack length. The morphology of ostial fibers resembles that of myocardial fibers. Interconnected bundles of myofilaments occur in both the ostial fibers and the myocardial fibers. In ostial and myocardial fibers, the myofilament bundles are invested by perforated sheets of sarcoplasmic reticulum, and these sheets interface with a network of sarcolemmal tubules to form dyadic interior couplings at the level of

the sarcomeric H-bands. The contractile apparatus originates and terminates at intermediate junctions on the transverse cellular boundaries, and the lateral surfaces of the muscle fibers are linked by a modest number of communicating (gap) junctions.

Key words Contraction · Heart · Ostium · *Homarus americanus* (Crustacea)

Abbreviation EPSP excitatory postsynaptic potential

Introduction

The heart of a decapod crustacean consists of a single ventricle located immediately under the carapace in the posterior half of the thorax. The ventricle is composed of striated muscle fibers (Sanger 1979; reviewed by Nylund et al. 1987) which are innervated by the cardiac ganglion located on the inner dorsal wall of the ventricle (Alexandrowicz 1932). The motoneurons of the cardiac ganglion branch extensively, and each muscle fiber receives multineuronal input (Anderson and Cooke 1971; Kuramoto and Kuwasawa 1980). Heart beat is considered to be neurogenic, because the myocardium is not spontaneously active (Maynard 1960).

Crustaceans possess an open circulatory system that lacks veins. After blood leaves the arteries and lacunar “capillary” spaces, it is channeled through defined sinuses and returns via the gills to the pericardial sinus in which the heart is suspended. In lobsters, blood returns to the ventricle through three pairs of ostia. The valves in the ostia, like the myocardium, contain striated muscle fibers which are innervated by the cardiac ganglion.

There is a large body of literature on the physiology of the cardiac ganglion (reviewed by Cooke 1988) and a growing literature on pumping mechanics and responsiveness of the intact heart to neurohormones (Wilkens and McMahon 1994; McMahon et al. 1997), but there is only limited information on the physiology of the myocardium (Hallett 1970; Van der Kloot 1970;

T. Yazawa
Laboratory of Neurobiology, Department of Biology,
Tokyo Metropolitan University, Minami-Ohsawa,
Hachioji 192-03, Japan

J.L. Wilkens (✉) · M.J. Cavey
Department of Biological Sciences,
University of Calgary,
2500 University Drive NW,
Calgary, Alberta, Canada T2N 1N4
e-mail: wilkens@ucalgary.ca
Tel.: +1-403-2206793; Fax: +1-403-2899311

H.E.D.J. ter Keurs
Department of Medicine
and Department of Physiology and Biophysics,
Faculty of Medicine, University of Calgary,
3330 Hospital Drive NW, Calgary, Alberta, Canada T2N 4N1

M.J. Cavey
Department of Cell Biology and Anatomy,
Faculty of Medicine, University of Calgary,
3330 Hospital Drive NW, Calgary,
Alberta, Canada T2N 4N1

Anderson and Cooke 1971; Anderson and Smith 1971). Our goal is to study the mechanics of contraction and the mechanisms of action of neurohormones on the myocardium removed from the neural drive from the cardiac ganglion. In our hands, isolated ostia contract strongly when electrically stimulated, while bands of myocardium contract only weakly. We propose that the ostia provide a model system for the study of the decapod myocardium, much as trabeculae are used as a model system for the study of mammalian myocardium. In this report, we describe the contractile properties and the basic morphology of the ostial muscles. Subsequent reports will address excitation-contraction coupling, the force-calcium relationships of these striated muscle fibers, and the signal transduction mechanisms that mediate peptide neurohormone actions.

Materials and methods

Lobsters (*Homarus americanus*) weighing between 470 g and 660 g were purchased from a commercial supplier and maintained in an artificial sea water system at 12 °C. Animals were fed frozen smelt weekly until used for experimentation.

Prior to surgery, lobsters were euthanized by rapidly destroying the brain by crushing the carapace between the eye stalks. To prepare the ostia, the posterior third of the dorsal cephalothorax with the heart was removed and placed in saline (Cole 1941), pH 7.6, at 4 °C. Ostia were dissected out and stored in aerated saline at 4 °C for up to 48 h. For experimentation, individual ostia were placed in a narrow Sylgard-lined chamber (1.5 ml). The saline volume was lowered to 0.3 ml during experiments to maximize electrical stimulating current. At all times, the bath was continuously superfused at 2 ml min⁻¹ with saline at 12–13 °C. During dissection of a valve, care was taken to neither touch nor manipulate the ostial leaflets. To obtain the strongest contractions, it was necessary to leave small pieces of myocardium attached to the ends of the ostium. To record contractions, an anchoring micropin was placed in one end of the valve lumen, and the pin of a mechanical transducer was placed in the other (Fig. 1). For force-length tension measurements, the transducer was moved by a micromanipulator so that stretch was applied at the point where the two leaflets join. It was found that anchoring pins placed in the pieces of myocardium left attached to the ends of an ostium would tear out before high levels of stress could be attained. Ostial muscles were electrically stimulated via a pair of laterally-placed electrodes (train stimulation of 2-ms pulses delivered at 30–120 Hz, variable train duration, variable train rate and suprathreshold voltage), while tension was measured by means of a Pixie force transducer (developed by R.K. Josephson and D. Donaldson; reported in Miller 1979) or SensoNor AE801 force transducer.

The membrane potential of in situ ostial fibers, innervated and driven by the cardiac ganglion, was measured from semi-isolated hearts by a hanging microelectrode technique (Wilkins and McMahon 1994). These electrodes were constructed by scoring the side of a standard 3-M KCl-filled long shank microelectrode just behind the bevel with a diamond etching tool, breaking the tip off and inserting a 0.05-inch diameter chlorided silver wire. The glass tip was secured to the wire by a droplet of melted wax. Electrodes of 10–20 Mohm tip resistance were used. Signals were recorded by a Nihon Koden amplifier (MEZ 8300), stored on a Teac MR-10 FM tape recorder and displayed on a Nihon Koden VC-11 digital oscilloscope at a sampling rate of 200 kHz. During these observations, the force produced by the intact heart was recorded by a Nihon Koden TB-612T force transducer that was attached by a small hook to the anterior ventral wall of the semi-isolated heart. Illustrations were produced by Nihon Koden data acquisition/

analysis software and printed on a Hewlett Packard ColorPro x-y plotter.

Morphology

To prepare tissues for transmission electron microscopy, ostia were pinned at slack lengths and at predetermined extended lengths to dental wax in a Petri dish and flooded with primary fixative [2.5% glutaraldehyde, 0.2 M phosphate buffer (pH 7.4), and 0.14 M sodium chloride] for 5 min. In some cases, fixative was poured directly onto the in situ heart immediately after removal of the overlying carapace, and the ostia were cut out of the organ after 5 min fixation. After stabilization in primary fixative, the isolated ostia were transferred to fresh fixative for a further 60 min at room temperature. Without rinsing, the ostia were immersed in secondary fixative [2% osmium tetroxide and 2.5% bicarbonate buffer (pH 7.2)] for 60 min in an ice-bath. Following a brief rinse in demineralized water, the specimens were dehydrated with a graded series of ethanol, transferred through propylene oxide, and infiltrated and embedded in Ladd LX-112 epoxy resin.

Thin sections (1 µm) were cut with glass knives on a Sorvall MT-2B ultramicrotome and stained with an alkaline solution of azure II and methylene blue (Richardson et al. 1960). The sections were viewed and photographed with a Nikon Optiphot compound microscope equipped with planachromatic objective lenses and a Nikon HFX-IIA photomicrographic attachment. The compound microscope was calibrated with a stage micrometer (100 lines mm⁻¹). Ultrathin sections (80 nm) were cut with diamond knives on a Sorvall MT-6000 ultramicrotome and stained serially with aqueous solutions of uranyl acetate (saturated) and lead citrate (Reynolds 1963). The sections were viewed and photographed with an Hitachi H-7000 transmission electron microscope operated at 75 kV. The electron microscope was calibrated with a carbon replica of a diffraction grating (2,158 lines mm⁻¹).

Statistics

Data are presented as means ± SD. Data were compared statistically by one-tailed or two-tailed *t*-tests ($\alpha = 0.05$).

Results

Anatomy

A drawing of the heart and the ventral pair of ostia appears in Fig. 1A. The ostial muscles are given the formal name *musculus orbicularis ostis* owing to their anatomical similarity to the *musculus orbicularis oris* that flatten the lips of the human mouth. Each ostium consists of a pair of leaf-like valves which fold into the lumen of the heart (Fig. 1B). A thin-walled cup borders each leaflet. A further band of muscle is located at the peripheral margin of each ostium. These latter bands are orientated at an acute angle to the long axis of an ostium, and each half resembles a “mustache” over the mouth-like opening. The muscle fibers of the valve leaflets, the thin cusp, and “mustache” are orientated in parallel to the long axis of a valve. All ostia appear to have the same basic morphology, but are of different lengths. The dorsal and ventral pairs are 6.66–8.88 mm in length while the lateral pair are 3.33–4.44 mm long in lobsters of the weight range used here. The ostia open during diastole to allow blood entry into the ventricle and close during systole to prevent back flow.

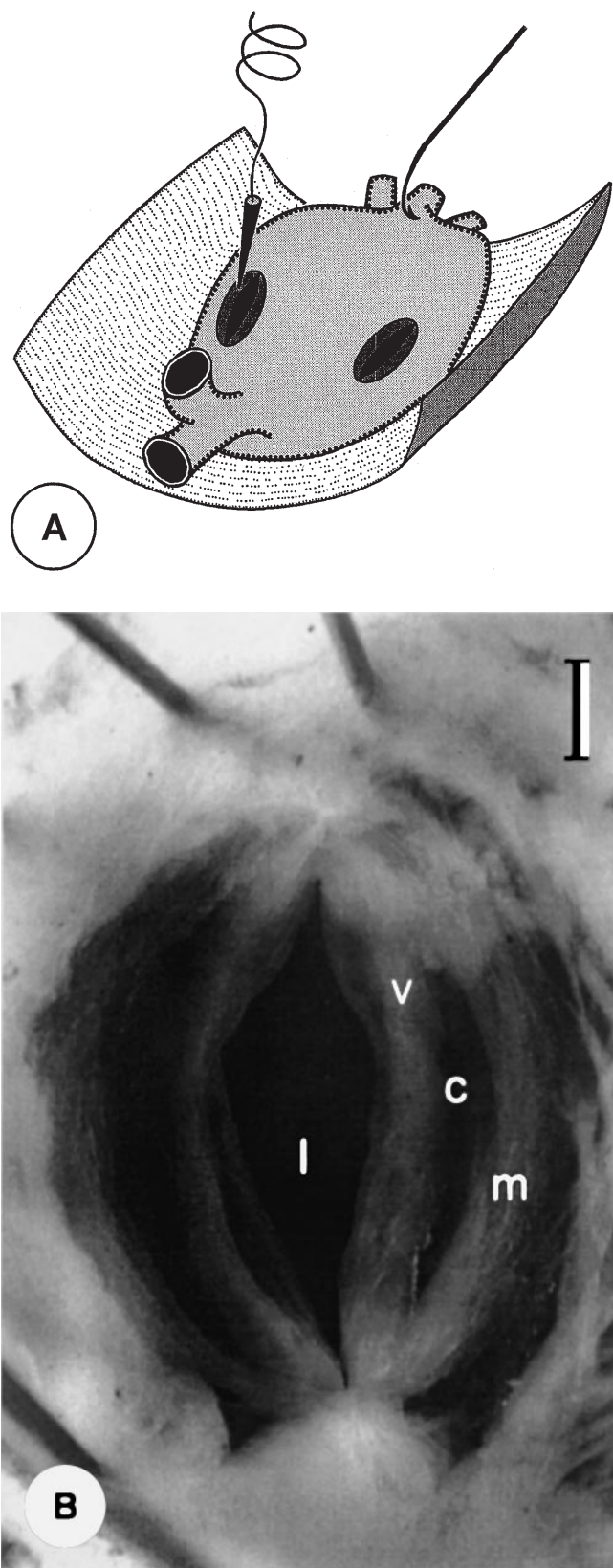


Fig. 1A, B Anatomy of the ostia. **A** Schematic drawing of a semi-isolated heart of *Homarus americanus* attached to a fragment of cuticle. Two ostia appear on the ventral surface of the heart, and one is impaled by a hanging electrode. A hook (attached to a force transducer) impales the anterior end of the heart. **B** Photomacrograph of the posterodorsal ostium, illustrating its lumen (*l*), valves (*v*), and cusps (*c*). Note the ostial "mustache" (*m*). Bar: 1 mm

Electrical and mechanical properties of the valve leaflets

The resting membrane potential of ostial muscles in intact spontaneously beating hearts, measured by a hanging microelectrode, was -52.4 ± 1.3 mV ($n = 11$). It was not possible to measure the force generated by in situ ostia during cardiac ganglionic-induced contractions, but it was assumed that the time course of the contractions was the same as that recorded from the whole heart. The fibers responded to a burst of action potentials from the cardiac ganglion with an excitatory postsynaptic potential (EPSP) that led to an action potential of up to 62 mV that often overshoot 0 mV, followed by a depolarizing plateau which arose from compound EPSPs (Fig. 2). The duration of the plateau corresponded to the duration of the burst of action potentials produced by the cardiac ganglion. Action potentials of similar amplitude were measured during direct stimulation; however, the stimulus artifact arising from the field stimulation made it difficult to record action potentials accurately. EPSP duration in hearts beating at 50 beats min^{-1} (cycle period of 1200 ms) was 300–400 ms and systole lasted 500–700 ms. The onset of force occurred at the time of the first spike of the

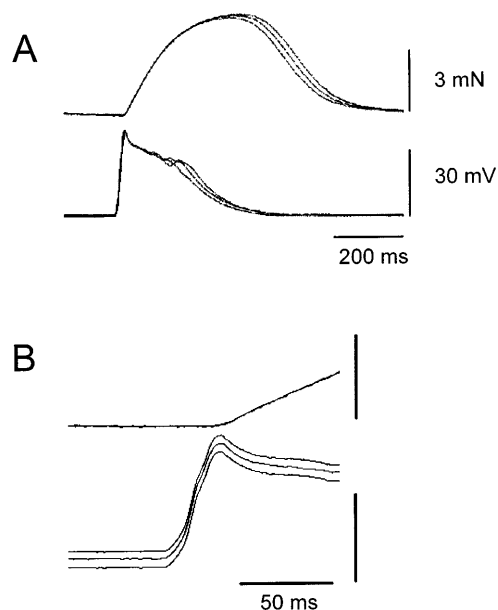


Fig. 2 **A** Three superimposed traces of membrane potential recorded from an ostial muscle fiber (lower traces) and the tension generated by an intact, spontaneously-beating heart (upper traces). **B** The same traces as in **A** displayed on an expanded time base. The three traces of membrane potential have been artificially offset

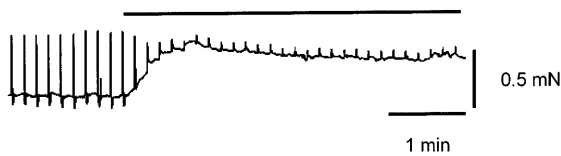


Fig. 3 Record showing electrical stimulation induced phasic contractions of an ostium before and during exposure to high-potassium (215 mM) saline as indicated by the bar over the trace

depolarization, and the amplitude and duration of the contraction increased with the duration of the EPSP. Depolarization of isolated ostia caused by saline containing elevated K^+ (210 mM) produced contracture (Fig. 3). Relaxation from this process was slow. The membrane potential was not measured during K^+ contracture, but electrical stimulation still caused small-amplitude phasic contractions.

Post-activation potentiation of contraction force occurred after a period of inactivity. Although this phenomenon has only been described for fast-twitch vertebrate muscle (Brown and Loeb 1988), post-activation potentiation was apparent in both freshly-prepared ostia and those stored overnight at 4 °C. The contractile force was very low at the beginning of a test period, but with regular stimulation (trains of stimuli of 2-ms pulses, 50–80 Hz, 300–500 ms train duration, 0.05–0.20 train s^{-1}), the contractions slowly became stronger, reaching a stable level after 90–240 min of continuous train stimulation (Fig. 4). Once contractile force had stabilized, it remained stable even after a 60–90-min rest period. Thus, all of the following data are collected from fully-potentiated muscles.

Summation of force, due to incomplete relaxation, was observed when trains of stimuli (50 Hz, 200 ms train duration) were delivered at a rate greater than 0.5 train s^{-1} (Fig. 5). Summation led to tetanus as train rate increased. Intra-muscle-fiber facilitation, seen as the increased amplitude of individual phasic contractions, occurred when the train rate exceeded 0.2 train s^{-1} . Force elicited by a 300-ms train duration (50 Hz) was augmented up to four times immediately following a brief tetanus (3 s train, 80 Hz) (Fig. 6). The time

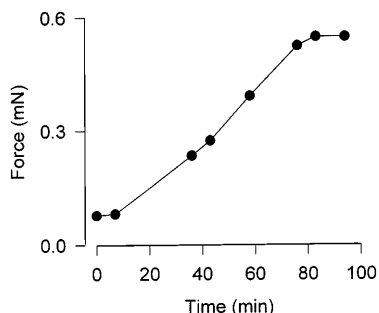


Fig. 4 Plot showing the development of post-activation potentiation of an ostium that was stimulated at a rate of 0.2 train s^{-1} (2 ms pulses, 80 Hz, 500 ms train duration). Prior to the onset of stimulation this ostium had been stored overnight at 4 °C

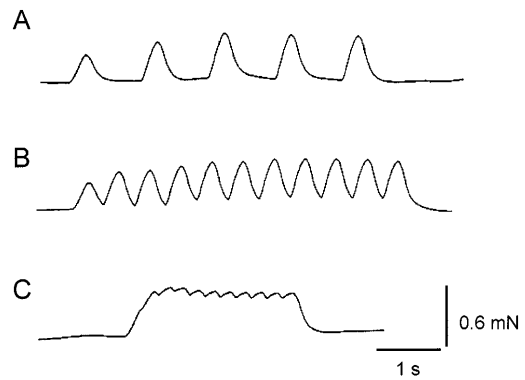


Fig. 5 Records of phasic contractions of an ostium in response to trains of stimuli delivered at one (A), two (B), and four (C) train(s) s^{-1} . Each train consisted of 2-ms pulses delivered at 50 Hz and 200 ms train duration

constant for the decay of intra-muscle-fiber facilitation, calculated from the time course of the ratio of the amplitude of the twitch following a brief tetanus divided by the twitch preceding it versus the time after the tetanus (facilitation index), was 5.6 s. A train rate of 0.05 train s^{-1} was used whenever facilitation was to be avoided.

Contraction amplitude increased sigmoidally with increasing pulse frequency reaching maximum force at 80–100 Hz (Fig. 7A). When the train rate (0.1 train s^{-1}) and pulse frequency (80 Hz) were held constant, force increased with increasing train duration, reaching a maximum at 500 ms (Fig. 7B). At high-stimulus intensities, electrolysis occurred at the stimulating electrodes, and the force of contractions declined during trains that were longer than 1000 ms, possibly due to O_2^- damage, an abrupt decrease in pH or to fatigue. This electrolysis-induced artifact may have contributed to the larger error bar for the 2000-ms point in Fig. 7B.

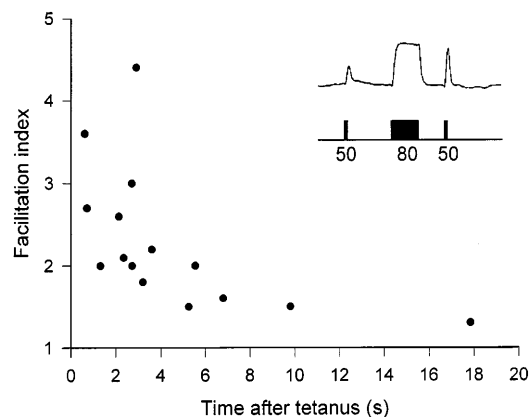


Fig. 6 Plot of the intra-muscle-fiber facilitation index, defined in the text, as a function of time after tetanus. Inset is a chart recording showing the experimental protocol, with tension in the upper trace and electrical stimuli in the lower trace. The two test trains consisted of 2-ms pulses delivered at 50 Hz for 300 ms; the tetanus consisted of 2-ms pulses delivered at 80 Hz for 3 s

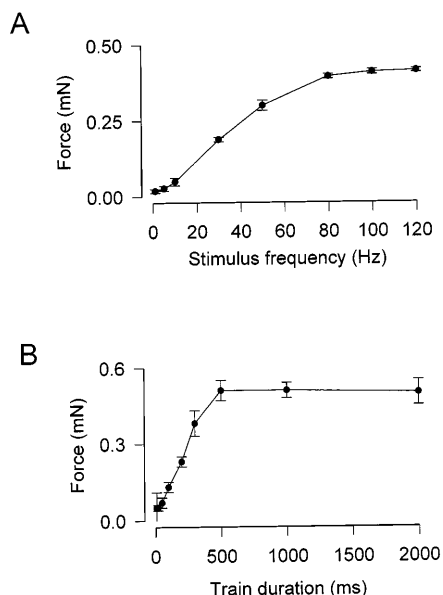


Fig. 7 **A** Force produced by an ostium as a function of the intratrain stimulus frequency during 300 ms trains (**A**). **B** Effect of stimulus train duration, 50 Hz pulse rate, on force produced by an ostium. Individual stimuli were 2 ms in duration, superthreshold, and train rate of $0.05 \text{ train s}^{-1}$

The force-length relationship for an ostium of 6.6-mm slack fiber length is illustrated in Fig. 8. The passive and active forces generated by the muscles were measured, starting from the slack length where tension was 0 and continuing until the muscle was stretched to ~130% of slack length. The actual force of the contractile components, obtained by subtracting the passive force from the active force, reached a maximum value at 1.2 times the slack length. The small difference between active force and passive force indicates that these muscles are relatively stiff. We could not measure

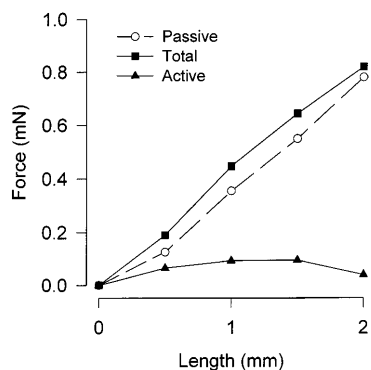


Fig. 8 Length-force relationship for a single ostium showing the passive tension in response to stretch, the total force in response to train stimulation, and the actual force which is the difference between the first two curves. The ostium was stretched from the slack length of 6.6 mm, the length where passive tension began to deviate from 0, to a length of ~130% of slack length. Trains of electrical stimuli consisted of 2-ms pulses, 50 Hz intratrain spike frequency, 300 ms train duration, delivered at $0.05 \text{ train s}^{-1}$

sarcomere length because we could not obtain laser diffraction patterns from the valve leaflets using the same apparatus used for rat cardiac trabeculae (ter Keurs et al. 1980).

There is physiological evidence, in addition to the morphological evidence presented below, that ostial muscle fibers are electrically coupled. Any damage to one side of the two leaflet valve reduced contractile force of the whole ostium by 40–75% (data not shown). Preparations reduced to a single valve leaflet did not contract when stimulated, and fura-2 injected into a single fiber spread laterally into adjacent cells (T. Shin-ozaki, J.L. Wilkens, T. Yazawa, M. Miura, H.E.D.J. ter Keurs, personal observation).

Morphology

Muscle fibers from an ostium (Fig. 9A) and those from the myocardium (Fig. 9B) share a number of ultrastructural characteristics. In both fiber types, the contractile apparatus forms a network of interconnected bundles of myofilaments (*Felderstruktur*) confined to the medullary sarcoplasm. The myofilament bundles are invested by regular dense perforated sheets of sarcoplasmic reticulum. Transverse tubules originate from invaginations of the sarcolemma. Longitudinal branches of these tubules form dyadic interior couplings with the sarcoplasmic reticulum at the level of the sarcomeric H-bands (Smith and Anderson 1972). Mitochondria are abundant in the cortical sarcoplasm, and they make close contacts with the sheets of sarcoplasmic reticulum at the periphery of the contractile apparatus. The myofilament bundles originate and terminate in intermediate junctions at the jagged transverse boundaries of the muscle fibers. A small number of communicating (gap) junctions link each muscle fiber to its neighbors.

Discussion

The inward-pointing arrangement of the ostial valve leaflets allows movement of blood into the heart during diastole and prevents backflow during systole. Contraction of the parallel-oriented muscle fibers will stiffen the leaflets in the closed position during systole. The ultrastructure of ostial muscle fibers resembles that of myocardial fibers (viz. branching configuration of the contractile apparatus, a high density of perforated sheets of sarcoplasmic reticulum, sarcolemmal tubules both in transverse and longitudinal orientations, dyadic couplings between sarcoplasmic reticulum and sarcolemmal tubules at the level of the sarcomeric H-bands and possibly at the Z-bands, intimate associations between mitochondria and sarcoplasmic reticulum, heavy glycogen accumulations in the vicinity of the contractile apparatus, intermediate junctions where the contractile apparatus originates and terminates, and communicating junctions between a muscle fiber and its neighbors).

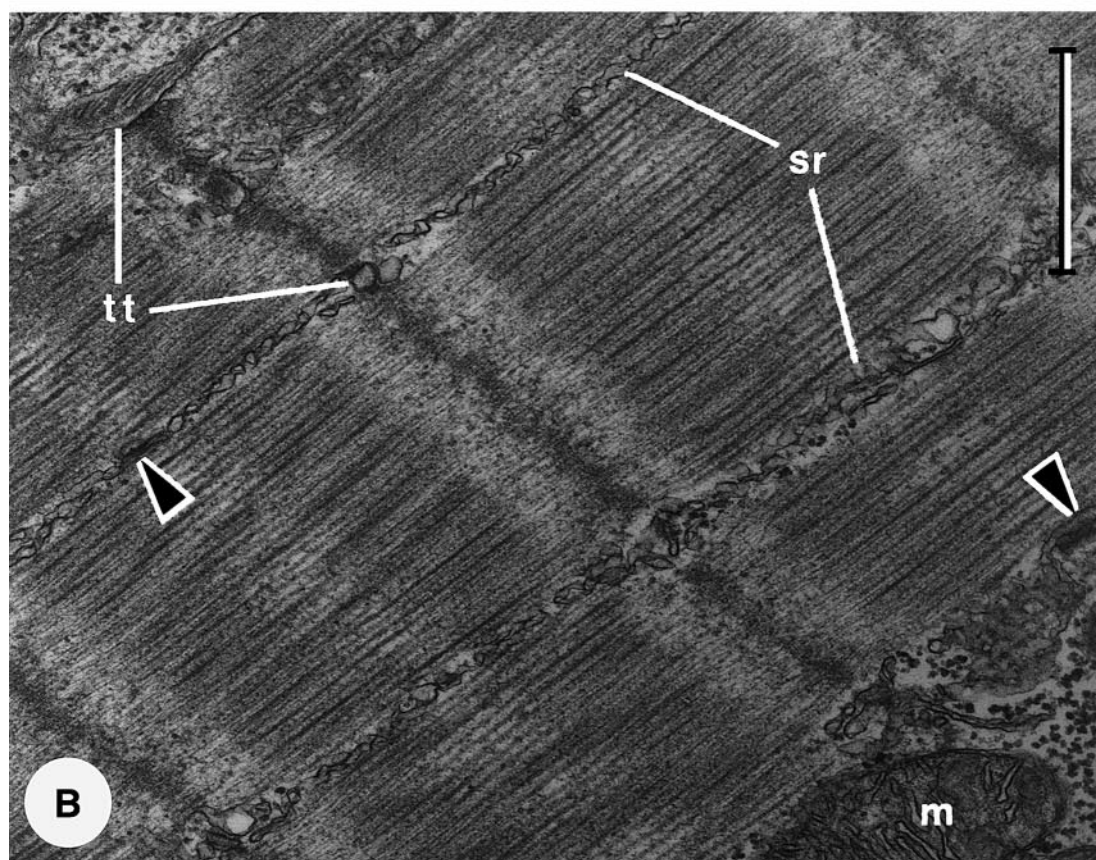
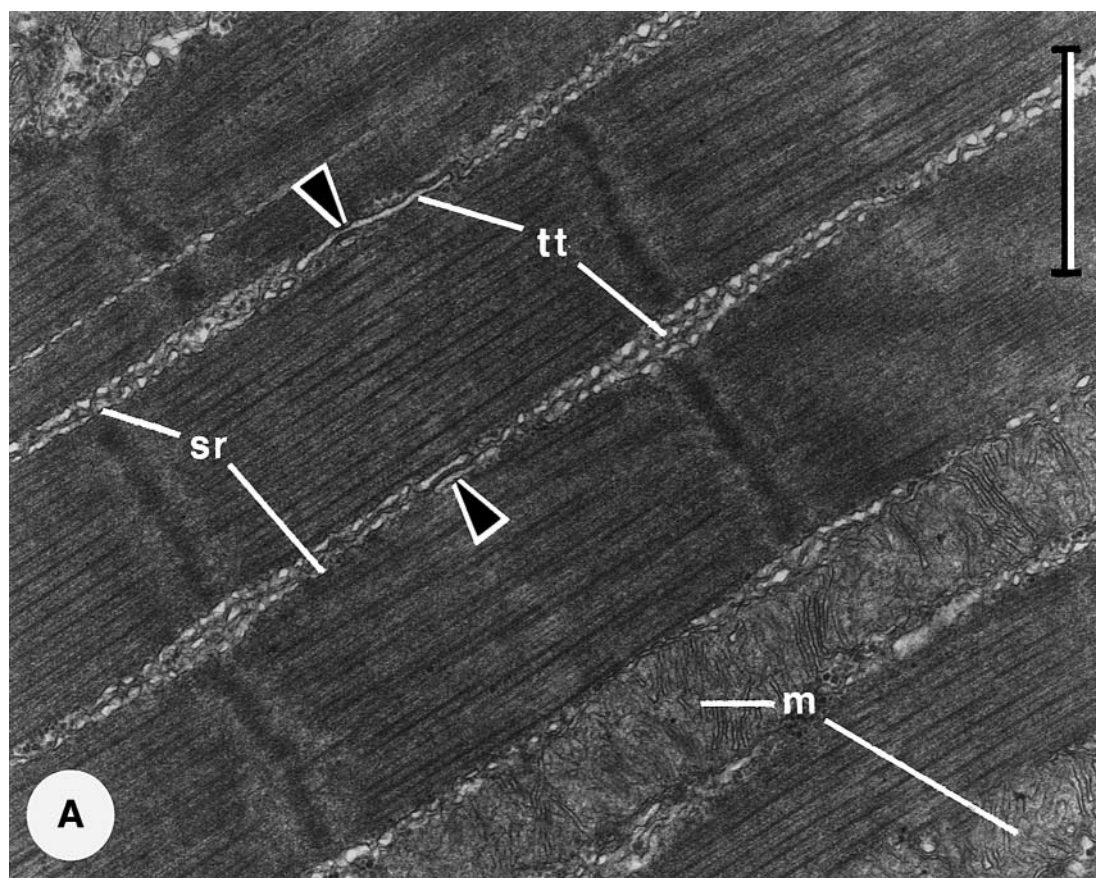




Fig. 9 Ultrastructural comparison of muscle fibers from an ostium (A) and from the myocardium (B) of the lobster heart. The myofilament bundles of an ostial fiber tend to be transversely striated, while those of a myocardial fiber have oblique striations. Sarcomeres of an ostial fiber are slightly longer than those of a myocardial fiber. In both fiber types, perforated sheets of sarcoplasmic reticulum (*sr*) surround the myofilament bundles. Transversely-oriented and longitudinally-oriented sarcolemmal tubules (*tt*) closely oppose the sheets of sarcoplasmic reticulum. Dyadic interior couplings (*arrowheads*) form between cisternae of the sarcoplasmic reticulum over the sarcomeric H-bands and longitudinal sectors of the sarcolemmal tubules; *m* mitochondrion. Bars: 1 μ m

The valve musculature and myocardium are innervated by the same motoneurons that originate in the cardiac ganglion.

Differences between the ostial and myocardial fibers are subtle. The contractile apparatus of an ostial fiber is transversely striated, while that of a myocardial fiber tends to be obliquely striated. Sarcomeres are slightly longer in ostial fibers than in myocardial fibers. A perforated sheet of sarcoplasmic reticulum generally invests each myofilament bundle in an ostial fiber, but in a myocardial fiber, adjacent myofilament bundles often share a single sheet of sarcoplasmic reticulum. Longitudinally-oriented branches of sarcolemmal tubules are more prominent in ostial fibers than in myocardial fibers. Mitochondria reside both outside and inside the contractile apparatus of a muscle fiber from an ostium; in the myocardium, mitochondria tend to be restricted to the periphery of the contractile apparatus of a muscle fiber (M.J. Cavey, T. Yazawa and J.L. Wilkens, personal observation). Due to extensive branching of and electrical coupling between myocardial fibers, it was impossible to prepare isolated bands of myocardium that contracted as well to direct electrical stimulation, as did the ostial muscles. Even though there are slight differences between the ultrastructure of the ostia and that of the myocardium, we feel that the ostia can serve as a good model system for the study of the lobster heart. There might yet turn out to be some, as yet undetected, type of terminal cisternal analog that would account for the observed contractile speed.

The “mustache” fiber bands that encircle the ostial leaflets have a sphincter-like configuration. They are in a position to functionally separate an ostium from the myocardium proper. Assuming that all fibers contract synchronously during systole, the contraction of the “mustache” bands will prevent any tendency for lateral tension arising from the myocardium from pulling the ostial leaflets open. Contraction of the “mustache” muscles would also allow the valve leaflets to slacken and move closer together. The contraction of the ostial muscle fibers will take up the slack and stiffen the leaflets and prevent the pocket of the valve cusp from extending and, thus, resist any systolic reflux of blood. During diastole, the relaxation of the “mustache” bands would allow lateral tension from the myocardium to pull the valves open.

It is generally supposed that lobster myocardial fibers are coupled electrically (Van der Kloot 1970; Hallett 1971). However, Anderson and Smith (1971) could not record electrotonic potential spread between adjacent fibers, did not observe lateral spread of procion dye between adjacent fibers, and did not find communicating junctions in their transmission electron micrographs. Anderson and Smith (1971) suggested that binding of procion to intracellular proteins prevented diffusion of the dye to the ends of fibers; the same explanation may also explain their failure to observe the lateral spread of dye. In the present study, morphological and functional evidence for communicating junctions is reported for the ostial muscle fibers. Communicating junctions are evident in our transmission electron micrographs. Electrical coupling between adjacent fibers may explain why damage to a single fiber will reduce or eliminate force generation by the affected valve and by the opposite leaflet. The reduction in force by one valve when the other is damaged suggests that the ends of the valve muscle fibers also contain communicating junctions where they meet. Fura 2 did diffuse into adjacent fibers on one valve leaflet and a small amount moved into the opposite leaflet as well.

The resting membrane potential of ostial fibers indicates that the fibers will relax completely during diastole. The EPSP response of the fibers to a burst of action potentials from the cardiac ganglion consists of an initial all-or-none muscle action potential that is followed by a plateau phase whose duration depends on the length of the motoneuron burst. Individual EPSP inflections are presumed to arise from individual motoneuron impulses, closely resembling the records presented by Anderson and Cooke (1971). The EPSP response is 300–400 ms in duration, and the final amplitude and duration of the period of force development increases with excitatory junction potential duration. If electrical and contractile properties of the myocardium are similar to those of the ostium, we predict complete relaxation during diastole and sub-maximal force development during ordinary cardiac ganglion-driven beating. We are currently measuring the magnitude and time course of the intracellular calcium levels ($[Ca^{2+}]_i$) during excitation by fura-2 fluorescence. Preliminary measurements indicate that during diastole, the $[Ca^{2+}]_i$ is below that which will initiate force and that $[Ca^{2+}]_i$ reaches maximal levels in response to 500-ms duration trains of electrical stimulation (T. Shinozake, J.L. Wilkens, T. Yazawa, M. Miura, H.E.D.J. ter Keurs, personal observation).

Post-activation potentiation in mammals occurs in fast-twitch muscle fibers (Brown and Loeb 1998). Its main effect is to enhance muscle force at sub-maximal activation levels for a short duration of time following previous muscle activation. One explanation for this phenomenon is the activity-dependent progressive phosphorylation of myosin regulatory light chains (reviewed by Sweeney et al. 1993). Ostial muscle that has been stored for several hours at low temperature

contracts weakly, but it becomes fully potentiated after a period of activation. It takes 60–90 min to develop full potentiation at the low stimulation rate used here ($0.05 \text{ train s}^{-1}$). In intact lobsters with a resting heart rate of $50 \text{ beats min}^{-1}$, the ostium, and presumably the myocardium as well, will be in a fully-potentiated state.

Facilitation of force development in a muscle that is stimulated via its motoneurons may represent the increase in the efficacy of the synapses as a result of the preceding activation of those synapses (Anderson and Cooke 1971). Intra-muscle-fiber facilitation also occurs due to events in the excitation-contraction coupling pathway that result in a greater calcium response (Hoyle 1983). The contractions of ostial muscles in response to 200-ms trains of electrical stimuli show intra-muscle-fiber facilitation at rates greater than 0.2 train s^{-1} . Assuming that the myocardium responds like an ostium, our data show that the long time constant for the decay of this facilitation (5.9 s) will contribute to contraction force by the heart even at the lowest heart rates (0.7 s^{-1}) observed in intact lobsters (Guirguis and Wilkens 1995). This facilitation, particularly at a high heart rate, may serve as an automatic regulatory mechanism to meet the increasing power requirements at elevated heart rates.

The force of contractions increased almost three-fold with increasing length. The total force curve has a peak at 30% stretch from slack length. Further stretch produced a decline of the actual force component (i.e., the difference between active and passive curves). The small difference between passive and active curves indicates that the ostial muscles are relatively stiff. The increases in force fit the observed pattern for vertebrate cardiac muscle (ter Keurs et al. 1980). When semi-isolated hearts are artificially stretched, the systolic pressures increase (Wilkens and McMahon 1994) indicating that the normal myocardial fiber lengths are shorter than the length which would generate peak force. The force-length relation in the lobster heart corresponds to the end-systolic pressure-volume relation in vertebrates, first described by Frank (1895) for the frog heart and later by Sagawa (1978) for the dog heart. Crustacean hearts have no veins and fill passively owing to recoil of the elastic alary ligaments during relaxation from systole. In addition, the heart can be stretched by the striated muscle fibers that occur in the alary ligaments (Volk 1988). Thus, diastolic volume is determined by the balance of elastic forces generated by the alary ligaments and of the cardiac wall.

Ultrastructural features of ostial muscle are suggestive of highly-aerobic, fatigue-resistant fibers. These muscle fibers exhibit well-developed systems of sarcoplasmic reticulum, transverse and longitudinal tubules of the sarcolemma, and extensive structural couplings between the longitudinal tubules and sarcoplasmic reticulum. Heavy concentrations of glycogen granules and abundant mitochondria with prominent cristae flank the contractile apparatus. The usefulness of ostial muscle as a model

system for study of the myocardium depends, in part, on the morphological similarities between muscle fibers from the ostium and those from the myocardium. The number of ultrastructural similarities already uncovered is encouraging.

Acknowledgements Ultrastructural components of this investigation were conducted in the Microscopy and Imaging Facility of the Faculties of Medicine and Science at the University of Calgary. Supported by a grant from the Natural Sciences and Engineering Research Council of Canada (JLW), Alberta Heritage Foundation for Medical Research and Medical Research Council of Canada (HEDJtK) and a private operating grant (MJC). All animal experiments complied with the guidelines of the Canadian Council of Animal Care.

References

- Alexandrowicz JS (1932) The innervation of the heart of the Crustacea. I. Decapoda. *Q J Microsc Sci* 75: 181–249
- Anderson M, Cooke IM (1971) Neural activation of the heart of the lobster *Homarus americanus*. *J Exp Biol* 55: 449–468
- Anderson M, Smith DS (1971) Electrophysiological and structural studies on the heart muscle of the lobster *Homarus americanus*. *Tissue Cell* 3: 191–205
- Brown IE, Loeb GE (1988) Post-activation potentiation – a clue for simplifying models of muscle dynamics. *Am Zool* 38: 743–754
- Cole W (1941) A perfusing solution for the lobster (*Homarus*) heart and the effects of its constituent ions on the heart. *J Gen Physiol* 25: 1–6
- Cooke IM (1988) Studies on the crustacean cardiac ganglion. *Comp Biochem Physiol C* 91: 205–218
- Frank O (1895) *Zür Dynamik des Herzmuskels*. *Z Biol* 32: 370–447 (Translated in *Am Heart J* 58: 282–317 and 467–478, 1959)
- Guirguis MS, Wilkens JL (1995) The role of the cardioregulatory nerves in mediating heart rate responses to locomotion, reduced stroke volume, and neurohormones in *Homarus americanus*. *Biol Bull (Woods Hole Mass)* 188: 179–185
- Hallett M (1971) Lobster heart: electrophysiology of single cells including effects of the regulator nerves. *Comp Biochem Physiol A* 39: 643–648
- Hoyle G (1983) *Muscles and their neural control*. Wiley, New York
- Kuramoto T, Kuwasawa K (1980) Ganglionic activation of the myocardium of the lobster, *Panulirus japonicus*. *J Comp Physiol* 139: 67–76
- Maynard DM (1960) Circulation and heart function. In: Wolvenkamp HP, Waterman TH (eds) *The physiology of Crustacea*, vol 1. Academic Press, New York, pp 161–226
- McMahon BR, Wilkens JL, Smith P (1997) Invertebrate circulatory systems. In: Dantzler WH (ed) *Handbook of physiology*, Section 13 (comparative physiology II). Oxford University Press, New York, pp 931–1008
- Miller TA (1979) *Insect neurophysiological techniques*. Springer, Berlin Heidelberg New York, pp 154–155
- Nylund A, Økland S, Tjønneland A (1987) The crustacean heart ultrastructure and its bearing upon the position of the isopods in eumalacostracan phylogeny. *Zool Scr* 16: 235–241
- Reynolds ES (1963) The use of lead citrate at high pH as an electron-opaque stain in electron microscopy. *J Cell Biol* 17: 208–212
- Richardson KC, Jarett L, Finke EH (1960) Embedding in epoxy resins for ultrathin sectioning in electron microscopy. *Stain Technol* 35: 313–323
- Sagawa K (1978) The ventricular pressure volume diagram revisited. *Circ Res* 43: 677–687

- Sanger JW (1979) Cardiac fine structure in selected arthropods and molluscs. *Am Zool* 19: 9–27
- Smith DA, Anderson ME (1972) The disposition of membrane systems in cardiac muscle of a lobster, *Homarus americanus*. *Tissue Cell* 4: 629–645
- Sweeney HL, Bowman BF, Stull JT (1993) Myosin light chain phosphorylation in vertebrate striated muscle: regulation and function. *Am J Physiol* 264: C1085–C1095
- terKeurs HEDJ, Rijnsburger W, Henuinger R van, Nagelsmit MJ (1980) Tension development and sarcomere length in rat cardiac trabeculae. *Circ Res* 46: 703–714
- Van der Kloot W (1970) The electrophysiology of muscle fibers in the hearts of decapod crustaceans. *J Exp Zool* 174: 367–380
- Volk EL (1988) The role of suspensory ligaments in modifying cardiac output in crustaceans. MSc Thesis, University of Calgary, Alberta
- Wilkens JL, McMahon BR (1994) Cardiac performance in semi-isolated heart of the crab *Carcinus maenas*. *Am J Physiol* 266: R781–R789

Communicated by L.C.-H. Wang